



Two-step-model of photosensitivity in cerium-doped fibers

TINO ELSMANN,^{1,*} MARTIN BECKER,¹ OLUGBENGA OLUSOJI,^{1,2}
SONJA UNGER,¹ KATRIN WONDRAKZEK,¹ CLAUDIA AICHELE,¹
FLORIAN LINDNER,¹ ANKA SCHWUCHOW,¹ JOHANNES NOLD,³ AND
MANFRED ROTHARDT¹

¹Leibniz Institute of Photonic Technology, Albert-Einstein-Strasse 9, 07745 Jena, Germany

²Abbe Center of Photonics, Albert-Einstein-Strasse 6, 07745 Jena, Germany

³Fraunhofer Institute for Applied Optics and Precision Engineering, Albert-Einstein-Strasse 7, 07745 Jena, Germany

*тино.elsmann@leibniz-iph.t.de

Abstract: The photosensitivity of various cerium-doped fibers has been experimentally investigated for both excimer- and femtosecond-laser illumination. The results of single-pulse, few-pulse and multi-pulse inscription of fiber-Bragg-gratings with both laser systems and the thermal aging of those gratings demonstrated the restrictions of the conventional color center model for cerium-doped fibers. To explain the short-term stability of single-pulse gratings against long-term stability of multi-pulse gratings, an extension into a two-step-model was deduced.

© 2019 Optical Society of America under the terms of the [OSA Open Access Publishing Agreement](#)

1. Introduction

The investigation on the photosensitivity of fibers was closely connected and triggered by the invention of fiber Bragg gratings (FBG) for the exploration of huge field of applications e.g. telecommunication or sensing.

The range of operation of all telecommunication and most sensing applications lies within the telecom C-band (around 1550 nm) and are mostly based on the use of germanium-doped fibers. Thus, a lot of studies on the photochemical process within germanium-doped silica glasses under illumination with UV-light lead to the discovery of different defects like the trapped electron centers (Ge(1) and Ge(2)), trapped hole centers (e.g. STH) or oxygen deficit centers [1–3]. Modification of these defect centers could lead to an increase in the photosensitivity of such fibers, different techniques have been employed to enact these process: hydrogen loading and high-germanium doping of the core are well-established methods [4,5], also, OH flooding, hypersensitization, or using of inscription laser at shorter wavelengths to enforce two-photon processes within the glass matrix are other valid techniques [6]. In various applications, the stability of the photo-induced structures for more than 25 years is a major factor to be considered [4], this spurred the development of theoretical models for the life-time predictions in germanium-doped fibers [7] as well as in hydrogen loaded fibers [8].

To make FBG readily available for the large market, an inscription technique was invented and optimized till industrial relevance: the draw-tower FBG. The concept of those kinds of gratings is based on the inscription of FBGs with only a single pulse of Excimer-laser during the fiber drawing process before the coating is applied [9–11]. Those gratings have the large advantage of possessing the same mechanical stability of the pristine fiber with mass production. Although they are limited in reflectivity due to the single inscription pulse, and the avoidance of the formation of damage gratings (so-called Type-II gratings) due to their non-reproducibility, broad spectral response and higher losses [11]. For draw-tower inscription, hydrogen loading is not an option. The practical way to guarantee a single-pulse grating with a reflectivity of

more than 30% is by doping with a higher concentration of germanium. Typically, fibers with 16 mol-% or higher are used, to enhance the photosensitivity as much as possible [4]. Using these high doping concentrations leads to a significant increase of the refractive index of the fiber's core, which leads to a conflict between single-mode regime and the mode-field-adaptation to standard fibers.

Since the invention of FBGs, other doping-elements aside germanium were explored. It has been demonstrated that the presence of cerium also enhances photosensitivity [12]. However, the photochemical processes in cerium-doped fibers was shown to be quite complicated [1,13], there were indications, that different defect species exist due to the vanishing of the gratings with different time constants ranging from minutes to days or the broadband modifications of the absorption spectrum. Notwithstanding, it was found, that the photosensitivity of cerium-doped fibers is based on the photo-excitation of Ce^{3+} -atoms, which can induce a 4f-5d shell-transition [14–18].

With our investigation, we demonstrated, that in cerium-doped fibers there is a huge difference between a single-shot and a multi-shot illumination caused by at least two different defect species with quite different properties. A comparison to standard-telecommunication-fibers and high-germanium-photosensitive fibers help to understand the necessary processes required to reach highly reflective gratings in cerium-doped fibers. A two-step-model was deduced from the experimental results, similar to the report for germanium-doped fibers [19,20].

2. Experimental setup

The inscription of the FBG in the fibers was carried out by a two-beam phase-mask interferometer using a frequency tripled femtosecond laser or a Krypton fluoride (KrF) Excimer-laser (see Fig. 1). The femtosecond laser emits pulses at a wavelength of 266 nm with pulse duration of 300 fs, intensity of 600 GW/cm²/pulse and a repetition rate of 1 kHz; while the KrF laser emits at a wavelength of 247 nm with pulse duration of 15 ns, intensity of 3 MW/cm²/pulse and a repetition rate of 1–30 Hz. The different focusing optics of these two laser systems enable them to have almost similar numbers of photons per pulse deposited in the fiber during the inscription process. Whereas the fs-laser provides those photons in a 50000x shorter time in comparison to the Excimer-laser, therefore other photo-chemical processes are possibly enforced [21].

The interrogation of the inscribed gratings was carried out with an erbium-doped Amplified Spontaneous Emission (ASE) broadband source with emission wavelength ranging from 1530 nm to 1570 nm and a Yokogawa 70D Optical Spectrum Analyzer (OSA) which allows the spectral scanning of the amplitude of the Bragg peak within a time interval of 100 ms (see also Fig. 1).

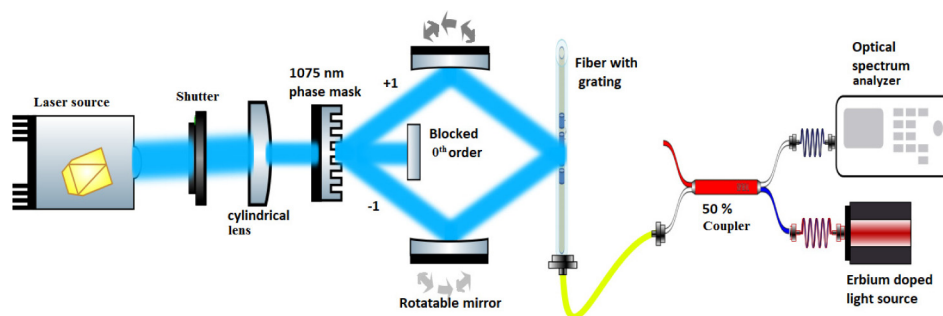


Fig. 1. FBG inscription and measurement setup

2.1. Characteristics of the fibers used for the interrogation

The study of the photosensitivity of cerium-doped fibers was carried out on different fibers that varied in both concentration and preform collapsing conditions, to isolate and specify the direct influence of those parameters on the grating formation. The fibers were fabricated in-house using the conventional MCVD process in combination with solution-doping (sol.-dop.) and gas phase doping technique (gas phase) for the incorporation of cerium and aluminum into silica glass matrix, followed by the fiber drawing technique.

The cerium concentration was varied in four steps from 0.04 mol-% Ce_2O_3 up to a maximum concentration of 0.53 mol-% Ce_2O_3 . This maximum limit was used in accordance to Dong et al. who showed the detrimental effect of having a dopant concentration above 0.58 mol-% Ce_2O_3 on photosensitivity [18]. Al_2O_3 and low amount of P_2O_5 were added to prevent cerium atoms from clustering and so to increase the solubility of the Ce into the silica matrix. These co-dopants also assist to reduce the formation of Ce^{4+} which produce readily available holes and reduces the photosensitivity of the fibers [18,22,23]. Additionally, the collapsing atmosphere was chosen to be reductive (He-atmosphere) or oxidative (Cl_2/O_2 -atmosphere) to influence the formation of Ce^{3+} and Ce^{4+} . The specific parameters of the various fibers used in the experimental analysis are shown in Table 1.

Table 1. Data sheet of the cerium-doped fiber.

fiber No	NA	Ce_2O_3 conc [mol-%]	P_2O_5 conc [mol-%]	Al_2O_3 conc [mol-%]	Production process	Collapsing atmosphere
1O	0.16	0.037	0.50	4.6	sol.-dop.	Cl_2/O_2
1R	0.16	0.036	0.50	4.5	sol.-dop.	He
2R	0.18	0.15	0.50	3.6	sol.-dop.	He
3O	0.18	0.34	0.50	4.3	sol.-dop.	Cl_2/O_2
3R	0.19	0.39	0.50	4.7	sol.-dop.	He
4O	0.19	0.53	0.50	4.8	sol.-dop.	Cl_2/O_2
4R	0.19	0.53	0.50	4.8	sol.-dop.	He
5O	0.12	0.06	nil	2.4	gas phase	Cl_2/O_2
6O	0.135	0.41	nil	1.6	gas phase	Cl_2/O_2

3. Theoretical background

The standard description of fiber-Bragg-gratings formation is based on the color center model, which was reported by Erdogan et al. [7] amongst other papers [24–27]. Other descriptions involves the densification model [28–30]. Within the densification model the UV exposure of the glass matrix results in a structural change and therefore, a densification of the glass. For the experimental conditions described within this paper the densification plays a secondary role [29,31]. The idea of the color center model is that electrons within the electro-chemical potential of the core material can be photo-excited. Those excited electrons reaching the conduction band can be trapped in a potential well of a color center (a defect within the glass matrix). For Ge-based fibers different defects mechanism were discussed. Kashyap [32] indicates, that an oxygen deficit center (ODC) absorbs the photons and forms an electron deficit center by donating an electron which can be caught in other defects within the neighboring glass matrix. While Nishii [1,33] argues that at first, a germanium-based electron center (GEC) is formed, which then relaxes to form a more stable germanium electron deficit center (GeE') [34].

Another approach to the chemical explanation is that of Erdogan's, which focuses on the mathematical description of the refractive index change based on the number of excited electrons. The dependence of temperature and time on the erasure/disappearance of the grating was

discussed with the assumption that the correlation between grating strength and excited electrons follows a Boltzmann-relationship. This leads to a power-law equation that shows the dependence of the grating strength on the time and temperature. The model can be expanded under the assumption of a variable reaction pathway [8,35,36] to a more general description.

Typically, the change in the refractive index Δn cannot be measured directly from the devices but it can be derived from the reflectivity R , which are correlated by

$$R = \tanh^2(\pi \cdot \Delta n \cdot l \cdot \eta / \lambda) = \tanh^2(ICC) \quad (1)$$

with l being the grating length, λ the Bragg wavelength and η the modal overlap parameter of the reflected mode respectively. In practice, the modal overlap parameter and the grating length are not exactly known but can be assumed to be constant for weak gratings with refractive index modulation below 10^{-4} in comparable fibers and the same FBG inscription routine. Therefore, the integrated coupling coefficient ICC is used which is only proportional to the refractive index modulation under the assumption of constant l , λ and η .

After the grating inscription, the color center electrons could be thermally depleted. This process starts from the electrons with the smallest energy difference in the undisturbed conduction band and continues by increasing energy difference till the electrons with imaginary depletion energy, known as demarcation energy, describes the physical age of the grating:

$$E_d = k_B \cdot T \ln(\nu \cdot t) \quad (2)$$

with k_B the Boltzmann constant, T the temperature, ν a normalization constant (depending on the material system) and t the time, respectively. Riant et al. [8] demonstrated that the ICC plotted against the demarcation energy becomes a line for a step-function of the potential well and the slope of this line indicates the depth of the well [8], which is the case for Ge-doped fibers. The logarithmic nature of the physical age of the grating underlines the importance of short term measurements during the FBG inscription with pulsed lasers.

4. Experimental results

4.1. Single-pulse grating – photosensitivity

The nine fibers out of Table 1, a SMF-28-like fiber and a high photosensitive Ge-doped fiber (18 mol-% Ge, without Ce, named high-Ge) were inscribed a few times with varying power of the fs-laser. The corresponding results (average of individual measurements) with error bars (standard deviation of individual measurements) are plotted in Fig. 2. The gratings are illuminated with 10 pulses instead of single pulses due to the limited aperture time of the applied mechanical shutter (10 ms). It will be shown in the section of multi-pulse inscription, that there is no significant difference between a 10-pulse and a single-pulse grating. Therefore those gratings will be called also single-pulse gratings throughout this paper.

Additionally, single-pulse gratings using the Excimer-laser were inscribed, but this system doesn't allow direct variation of intensity. To change the photon number reaching the fiber core, the position of the focusing lens was adjusted, to tune the focal width and therefore the intensity at the fixed position of fiber within the inscription setup. But it was discovered, that the lens aberration directly influences the contrast of the writing fringes which depends on the varying focusing conditions and this also affect the measured reflectivity of the gratings. This overlaying effect made the interpretation of the received results difficult, but they seem similar to the fs-laser results.

Under exposure of the different cerium-doped fibers to UV, a bluish fluorescent became observable. A part of the fluorescence light was guided within the core of the fibers, which could be measured with a spectrometer. The maximum of the detected fluorescent light was around 430 nm with a red-shift for higher doping concentration, resulting from stronger reabsorption of

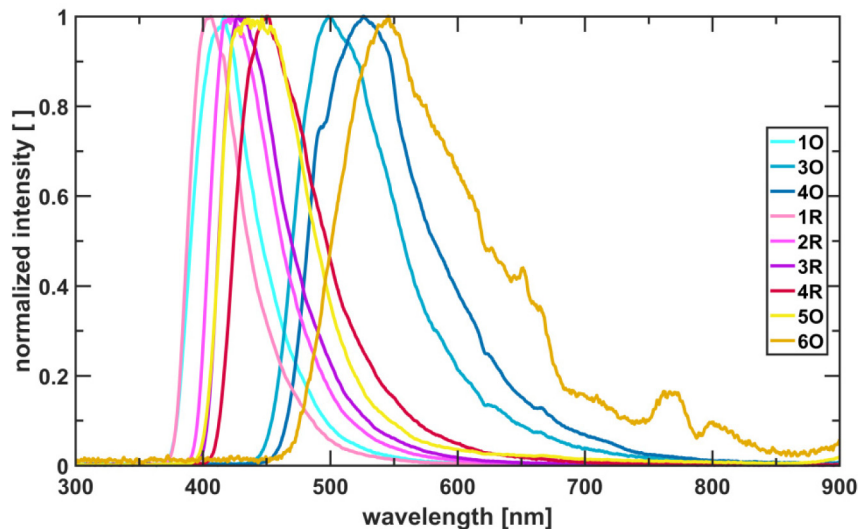


Fig. 2. Normalized fluorescence spectra of the fibers under UV-exposure. The light is measured through the core of the fibers.

shorter wavelengths during the propagation along the fiber core (see. Fig. 2). This fluorescent light is related to the 5d-4f-shell transition of Ce^{3+} [17], which corresponds to the measurements at the cerium-doped fibers and the description of the roll of cerium in photodarkening effect [37,38]. Therefore, the Ce^{3+} gets excited to Ce^{3++} forming a hole trapping center with the excited electron supposedly in its vicinity. By following this theory, the excitation into color centers is the major mechanism of UV-exposure [14,15,17,18], nevertheless, this chemical process is not yet fully understood, also other contributions to the FBG formation like densification or the influence of other co-dopants have to be discussed.

Plotting the ICC of single-pulse gratings inscribed by the femtosecond laser against the inscription power (Fig. 3), it can be noted, that the ICC increases for an increasing power of up to 200 mW, it implies that more electrons are trapped in the color centers due to fact that more photons hit the fiber core, under the assumption that the excitation of Ce^{3+} is the major underlying mechanism. For inscription power above 200 mW, there is no further increase of ICC within the typical uncertainty of 0.16 until 0.24 depending on the individual fiber. The saturated ICC is in the order of 0.6. For a grating length of 8 mm, an η of 0.8 and a λ of 1550 nm in correspondence to the experimental conditions the modulation of refractive index can be calculated by Eq. (1) to be 4.6×10^{-5} . The power independency of ICC above 200 mW is equivalent to the fact that, more photons do not excite more of the permanently deposited electrons. Within the proposed model of Erdogan, this can be only connoted to the fact, that the potential well is fully filled and therefore further excited electrons cannot be trapped.

Furthermore, no significant differences between the different dopant levels or collapsing atmospheres were denoted. However, there is a significant difference between the solution doped and the gas-phase doped fibers. The solution-doped fibers show a higher photosensitivity compared to gas phase-doped prepared fibers. The cause of this difference in behavior are currently unclear. Possible reasons could be the chlorination process or the presence of phosphorus as an additional co-dopant in the solution doping process, were considered. Although, those influences are not yet exhaustively investigated at the moment.

Remarkably, all the cerium-doped fibers exhibited a relatively high single-pulse photosensitivity in comparison to the germanium-doped fibers. The solution doped cerium containing fibers typically have a larger change in the refractive index with a factor of five in comparison to the

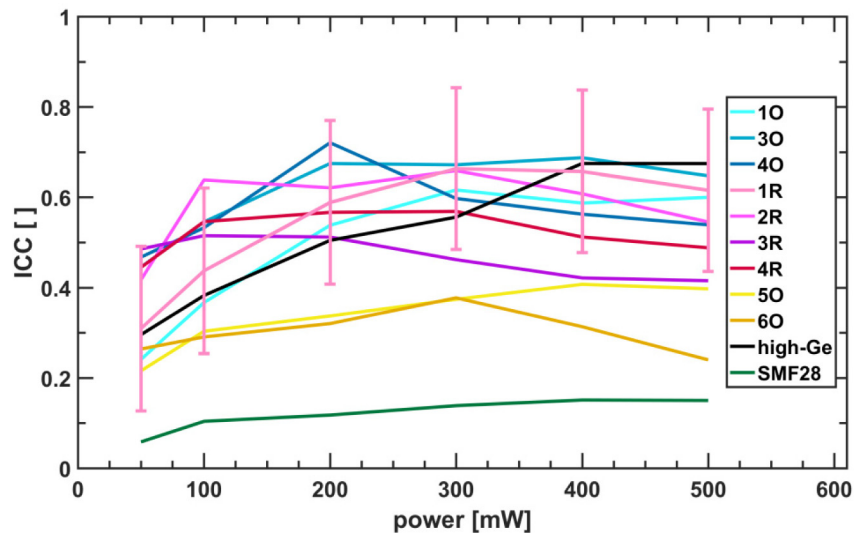


Fig. 3. Power dependency of ICC for femtosecond single-pulse gratings in different fibers. The error bars are similar for all fibers and are therefore indicated for one sample.

standard telecommunication fiber. Furthermore, there is a small amount of phosphorous and aluminum in the order of the GeO_2 -amount in the SMF28 fiber. Literally, the photosensitivity of these co-dopants can be assumed to be less than that of germanium [39,40], that is, their contribution to high photosensitivity of the cerium-doped fibers is secondary. The fibers even competed with highly photosensitive Ge-doped fiber with a factor of 500x smaller amount of dopants - 0.036 mol-% Ce_2O_3 against 18 mol-% GeO_2 .

4.2. Single-pulse grating – thermal stability

One special property observed in all the investigated Ce-doped fibers gratings was that: they decayed immediately after the inscription at room temperature. This behavior opposes the long-term stability of gratings in Ge-doped fibers over several decades of years at room temperature [7] but is in well agreements of literature [38]. The maximum reflectivity of the gratings with the evolution of the continuous reduction in the reflectivity was measured directly after the ten pulses of the femtosecond laser reached the fiber. To observe this effect more qualitatively, the automatized fast measurement routine of the OSA was used. In this mode, it measures only the maximum value within the given spectral range. To speed up the measurement, the bandwidth of the optical span, the slit width and the sampling point number were optimized (2 nm, 50 pm, 201 points). This lowered the interval of measurement to roughly 100 ms. The comparison in the decay of the fibers is shown in Fig. 4.

The grating drops around 45% of its initial strength within minutes until the first hour. The reduction in grating strength during the following two days is then less than 0.3% with the tendency to stabilize much more within the third day.

Using the representation of normalized ICC against the logarithm of time (normalized by 1 Hz), which is analogous to the demarcation energy, the decay is not perfectly linear as reported for Ge-doped fibers [8] but quite similar. The change of slope can be explained by the orbital splitting of the 5d orbital as reported by Ebendorff-Heidepriem [16], which causes an energetic sub-structure of the present defect.

The solution-doped fibers have similar behavior with a slight indication, that a higher dopant-concentration enhances the fast decay. This is more prominent in the gas-phase doped fiber with high Ce-concentration which decays faster than the others. This could be related to the

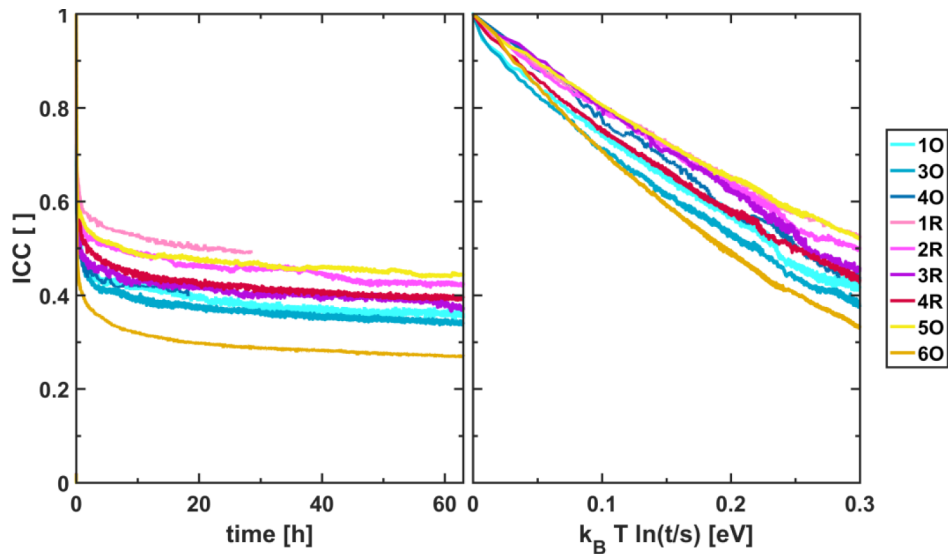


Fig. 4. Thermal decay of femtosecond laser inscribed gratings at room temperature. The grating strength – normalized to its initial value – drops down immediately after the inscription (left side), which is the result of an almost linear decrease of ICC against the logarithmic time scale analogous to demarcation energy (right side).

clustering of the cerium within the fiber core, with a tendency of a faster decay for higher doping concentration.

4.3. Multi-pulse grating – photosensitivity

For multi-pulse photosensitivity investigation, the Excimer-laser with a repetition rate of only 10 Hz and the femtosecond laser system (fs-laser) with its 1 kHz repetition rate were both used since they address different timescales. The fast relaxation of the single-pulse gratings, were observed to be within the timescale of Milliseconds. To investigate the influence of the high repetition rate of the femtosecond laser system, which is within the same time scale of the fast relaxation process, the fs-laser was used in two modes in comparison to the Excimer-laser. One mode is the so-called continuous mode, where the shutter is opened consciously and the fiber is illuminated with a repetition rate of 1 kHz. The other one is the burst mode, where the shutter is only opened every other second for 10 ms, which results in an averaged repetition rate of 5 Hz. To make the gratings comparable, all the fibers were illuminated with 4000 pulses, resulting in different inscription times for the three different modes of inscription.

The OSA was set to measure the reflectivity continuously, so that the timescales of the different inscription modes was scaled to make them comparable. The reflectivity was evaluated as a function of the illuminating pulses. The values are discretized due to the higher repetition rate of the laser when compared to the measurement speed for the fs-inscription (see Fig. 5). Only the fibers 3O and 3R with an intermediate Ce-concentration were used, because previous experiments indicate that no significant difference in the photosensitivity properties exist between the different solution-doped fibers.

The final amplitude of refractive index change in the fibers after 4000 pulses is quite similar for all the three different inscription methods. Additionally, no difference in the behavior of fiber 3O and 3R was observed, which is consistent with the previous results.

However, the way the final grating reflectivity was reached differs; especially for the continuous fs-laser illumination (4000 pulses in 4 s). The gratings show a much weaker growth over the 4000

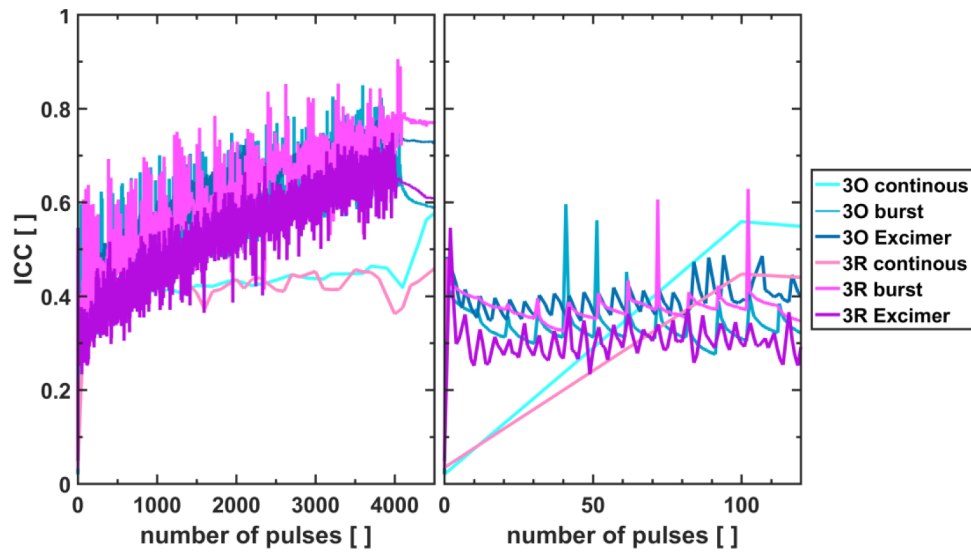


Fig. 5. Accumulation of reflectivity for illumination with 4000 pulses (left side) and the zoom-in for the first 120 pulses (right side). The femtosecond laser was used in a continuous and a burst mode, whereas the Excimer-laser was used only in a continuous mode.

pulses and a sudden reflectivity increase after the shutter was closed. The smoothness of the curve is attributed to the repetition rate of the fs-laser with a factor of 100 faster than the cycle time of the OSA. Therefore only an averaged spectrum could be measured with nearly no information of the pulse-to-pulse growth. The final jump of the ICC after the shutter was closed indicates a thermal chirp during the inscription which vanishes after the inscription. Thermal chirp means an inhomogeneous temperature profile within the grating region due to the Gaussian-like fs-laser beam profile and the accumulation of heat caused by the high repetition rate.

The other two inscription modes reveal more information because, the OSA is not averaging but measuring the reflectivity change for every individual pulse. They show strong fluctuation of the ICC under illumination. A zoom in to Fig. 5(left side) shows that, for every individual pulse or 10-pulse-sequence, a fast, positive ICC jump occurs, which immediately decreases afterwards. From pulse to pulse or sequence to sequence there is only a very weak residual contribution to the ICC growth. The residual ICC growth is that weak, that no difference between the real single-pulse and the 10-pulse sequence was found within 200 pulses. This means that the results of 10-pulse gratings are also representative of the single-pulse gratings. The residual ICC grows continuously over the 4000 pulses and becomes the dominant portion of the final ICC. This observation was obvious after the shutter was closed. A final fast decay of ICC from the last pulse was measured, but the residual ICC-value did not decay significantly within the next minutes and hours. Even after a long-term storage over 60 hours at room temperature, no decay in the ICC was observed contradicting the behavior of single-pulse gratings.

4.4. Multi-pulse grating – thermal stability

The stable reflectivity after the inscription indicates that the residual accumulated ICC has a much higher thermal stability than the single-pulse ICC. To demonstrate this, a 4000-pulse FBG within fiber 3R was thermally treated within a furnace and was compared with a 4000-pulse grating within the highly germanium-doped fiber. During the thermal treatment, the temperature was increased in 50 K steps from 100°C up to 400°C with a holding time of 2 h at every temperature step. The reduction in the normalized ICC is presented in Fig. 6(a).

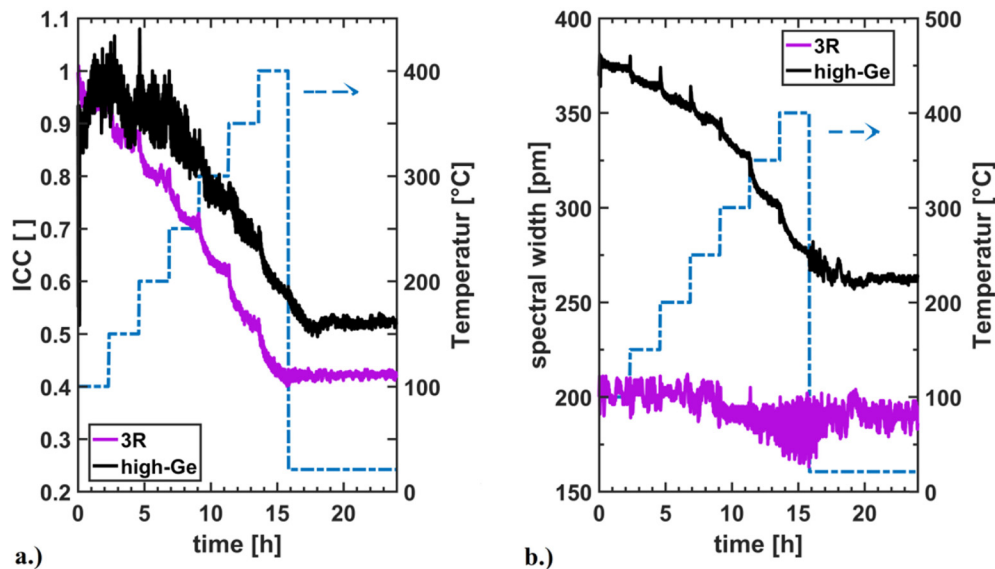


Fig. 6. a.) Thermal decay of grating (4000 pulses of fs-laser) in cerium- and germanium-doped fiber under thermal treatment. b.) Corresponding spectral width of the FBGs (4000 pulses of fs-laser) under thermal treatment. The dashed line indicates the aimed temperature profile.

Both fibers show a decay, which is always fast at the beginning of a new thermal level and slows down during the holding time. This agrees well with the theoretical description. The grating within the fiber 3R seems to have a little stronger comprehensive decay than those in the highly germanium-doped fiber. The slower decay of the comparison grating can be explained by the measurement method itself, as both gratings were monitored for their reflectivity. However, the 4000-pulse grating in the highly germanium-doped grating was an extremely high reflectivity grating (typically -40 dB in transmission). A consequence of saturation behavior and the mathematical form of the tanh-function (see Eq. (1)) is that, a significant decrease in ICC is not well measured as a change in reflectivity but as a change in the spectral width. For the representation in Fig. 6(a), the ICC was calculated out of the measured reflectivity. The behavior is different, if the spectral width is evaluated (see Fig. 6(b)).

The FBG within the Ge-doped fiber shows a much higher spectral width with 380 pm as compared to the Ce-doped fiber with 210 pm due to the high refractive index change. Under the previous described thermal treatment, this spectral width reduces by 120 pm, whereas only a reduction of 10 pm could be observed for the FBG in the Ce-doped fibers.

Comparing the Bragg wavelength shift between the initial gratings and the thermally treated gratings at room temperature indicates the modification of averaged refractive index within the FBG. The shift falls within the accuracy of the OSA (± 50 pm) with a decrease of 155 pm for fiber 3R and 176 pm for the germanium-doped fiber.

Concluding from these observed behaviors, the thermal stability of the residual ICC after 4000-pulse illumination within the cerium-doped fibers is comparable to that in a germanium-doped fiber.

5. Discussion

The single-pulse FBG inscription experiments, reveal a remarkable high photosensitivity of cerium-doped fibers compared to germanium-doped fibers. They attained the same maximum ICC even with a dopant concentration that is 500 times smaller. This behavior can be well

understood in the physical and chemical picture of the color centers by assuming that densification and the contribution of other co-dopants plays a minor role. To change the refractive index of the fiber, single electrons must be relocated within the glass matrix. For germanium-doped fibers, the electrons are strongly linked to the germanium ions, a complete change of the chemical bonds is necessary to relocate the electrons. However, cerium in the cerium-doped fiber are network-modifier, therefore, they not well linked within the glass matrix. Hence, the outer electron of the 4f-orbital is well shielded from the rest of the cerium and it's easier to excite it into the 5f-shell in comparison to the case of germanium.

Furthermore, saturation with increasing intensity was observed. In the color centers formation picture, more photons would result in the trapping of more electrons in the color center till they are saturated. This implies that the color center excitation within the Ce-doped fiber is reached at 200 mW for our inscription setup.

Single-pulse gratings in Ce-doped fibers start to vanish immediately after the inscription even at room temperature, which contrasts with the long-term stability of gratings in Ge-doped fibers, under the same conditions. Using the conventional color center model again, this means, that the Ce-based color center itself is more or less directly located at the conduction band (see Fig. 7), while for Ge-defects an energy gap of 2.7 eV is reported [8]. Hence, the excited electrons within the Ce-doped fibers can thermally relax easily as compared to Ge-defects.

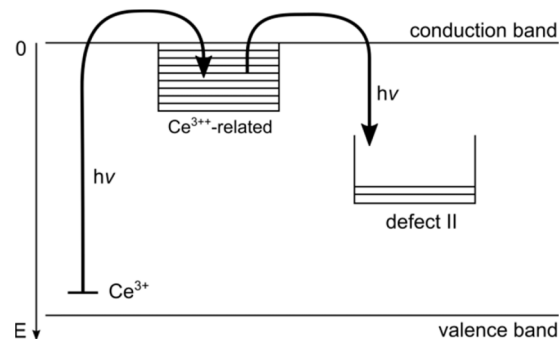


Fig. 7. Diagram of the proposed defect structure of the cerium-doped fiber.

This means that the positive effect of high photosensitivity is conflicting with the energetic position and form of the color centers, resulting in a strong but fast decaying gratings. This would restrict a large field of applications.

However, those results cannot be subjected to the multi-pulse inscribed gratings, which attained reflectivity, higher than the single-pulse gratings. Our experiments showed a steady grating growth and an improved thermal stability for multi-pulse gratings. The fact that for every individual pulse, the fast increase of ICC and a following fast decay similar to a single-pulse grating, is of importance. The obvious difference is that, a residual reflectivity or ICC accumulates very slowly from pulse-to-pulse over several hundred of pulses. This growth indicates the presence of at least, a second process/mechanism. The first one is the fast mechanism obtained in the single-pulse process, which was described above as a fast saturating process, with a potential well close to the conduction band. Furthermore, every additional pulse transforms a small amount of those excited electrons into a more thermally stable defect, which should be at a larger distance from the conduction band (see defect II in Fig. 7), exhibited as the residual growth of ICC. The comparison of the thermal stability with FBGs in Ge-doped fibers indicates an energy difference of a few eV, from this second defect to the first defect or conduction band.

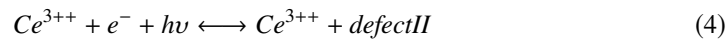
In contrast to the conventional color center model proposed by Erdogan [7], who discussed the photo-excitation process as one single process, where the electron is excited over the band-gap

and trapped in the color center; it was demonstrated that, for the cerium-doped fibers, the photo-excitation process should be separately discussed as two individual processes. In general, the change of the refractive index is related to a change of absorption by Kramers-Kronig-relation. Therefore, the absorption of the material, that is, the electrons state, has to be changed permanently and this doesn't have to be in one step compulsorily.

The first step is the excitation of an electron, identified as the Ce^{3+} excitation to a Ce^{3++} (which differs from a Ce^{4+} [41,42]). The dominant phenomenon of the fast relaxation of the excited electrons is given by this initial state.

The second step is the transformation to a permanent modification of the glass matrix. To achieve the desired permanent change of refractive index, the excited electrons should be separated energetically from its initial state. This can happen as a modification of a chemical bond or by spatial separation due to the movement of the photo-excited electrons within the glass matrix. An efficient photosensitive system comprises of both concepts: a well excitable initial state and an electron trapping mechanism.

For the cerium-doped fiber, the excited electron from the Ce^{3+} has to be removed and caught inside the glass matrix. It can be assumed that, the glass matrix itself stores the excited electron within other defect centers or rather modifies defects which are related to the silica glass matrix itself – e.g. E' , HC1 and HC2 [43] or the co-dopants. This could explain why only a limited number of excited cerium electrons are transformed into the long-term stable second defect. We assume the following chemical modification as the not yet identified *defect II*.



6. Conclusion

Cerium-doped silica fibers show an extreme high single-pulse photosensitivity, which allows a reduction of dopant concentration by a factor of 500 compared to conventional germanium-doping and therefore enhances the mode field adaption between high-photosensitive sensing fibers and standard telecommunication fibers. To make use this advantage, it becomes necessary not only to excite the electrons efficiently, but to also trap them within the glass matrix.

The behavior of the photosensitivity in cerium-doped fibers can be explained by a two-defect model, by assuming a minor influence of densification or the photosensitivity of the co-dopants. Within the two-step-model every individual laser pulse excites the outer 4f-electrons of cerium atoms into a fast-saturated defect, which is positioned close to the conduction band. Some of those electrons can be caught in a much deeper potential well, creating a thermally more stable second defect. Implying that, the multi-pulse gratings within the cerium-doped fibers can be used in similar fashion to gratings within standard germanium-doped fibers.

Our results indicate more generally that for an efficiently high-photosensitive fiber, two conditions have to be fulfilled. It is necessary to provide an easy excitation of electrons by photon interaction and it is also important to trap those electrons efficiently insight the glass matrix, to avoid a fast recombination of these photo-excited electrons. The cerium-doped fibers show a very efficient fast step of photo-excitation but an inefficient storage process in deep lying potentials. The understanding of the introduced two defect model helps to improve the design of highly photosensitive fibers.

For a better understanding of the influence of other photosensitivity contributions (co-dopants, densification) and reaction pathways, photoluminescence or optical absorption measurements can be used to extend the physical and chemical understanding. An expansion to the VAREPA-model can also improve the understanding of the underlying processes.

Funding

Free State of Thuringia (2015 FGR 0108).

Acknowledgment

The project on which these results are based was supported by the Free State of Thuringia under the number 2015 FGR 0108 and co-financed by European Union funds within the framework of the European Social Fund (ESF).

References

1. J. Nishii, K. Fukumi, H. Yamanaka, K. I. Kawamura, H. Hosono, and H. Kawazoe, "Photochemical reactions in GeO₂-SiO₂ glasses induced by ultraviolet irradiation: Comparison between Hg lamp and excimer laser," *Phys. Rev. B* **52**(3), 1661–1665 (1995).
2. T. Tsai, D. L. Griscom, E. J. Friebele, and J. W. Fleming, "Radiation-induced defect centers in high-purity GeO₂ glass," *J. Appl. Phys.* **62**(6), 2264–2268 (1987).
3. L. Griscom David, "Optical Properties and Structure of Defects in Silica Glass," *Ceram. Soc. Japan* **99**(1154), 923–942 (1991).
4. A. Othonos, "Fiber Bragg gratings," *Rev. Sci. Instrum.* **68**(12), 4309–4341 (1997).
5. A. Othonos and K. Kalli, *Fiber Bragg Gratings: Fundamentals and Applications in Telecommunications and Sensing*, Artech House Optoelectronics Library (Artech House, 1999).
6. M. Lancry and B. Pommellec, "UV laser processing and multiphoton absorption processes in optical telecommunication fiber materials," *Phys. Rep.* **523**(4), 207–229 (2013).
7. T. Erdogan, V. Mizrahi, P. J. Lemaire, and D. Monroe, "Decay of ultraviolet-induced fiber Bragg gratings," *J. Appl. Phys.* **76**(1), 73–80 (1994).
8. I. Riant and B. Pommellec, "Thermal decay of gratings written in hydrogen-loaded germanosilicate fibres," *Electron. Lett.* **34**(16), 1603 (1998).
9. C. G. Askins, T. Tsai, G. M. Williams, M. A. Putnam, and M. Bashkansky, "Fiber Bragg reflectors prepared by a single excimer pulse," *Opt. Lett.* **17**(11), 833–835 (1992).
10. L. Dong, J. L. Archambault, L. Reekie, P. S. J. Russell, and D. N. Payne, "Bragg gratings in Ce³⁺-doped fibers written by a single excimer pulse," *Opt. Lett.* **18**(11), 861 (1993).
11. C. Chojetzki, M. Rothhardt, J. Ommer, S. Unger, and K. Schuster, "High-reflectivity draw-tower fiber Bragg gratings — arrays and single gratings of type II," *Opt. Eng.* **44**(6), 060503 (2005).
12. L. Dong, P. J. Wells, D. P. Hand, and D. N. Payne, "Photosensitivity in Ce³⁺-doped optical fibers," *J. Opt. Soc. Am. B* **10**(1), 89 (1993).
13. H. Hosono, M. Mizuguchi, H. Kawazoe, and J. Nishii, "Correlation between Ge^{E'} Centers and Optical Absorption Bands in SiO₂:GeO₂ Glasses," *Jpn. J. Appl. Phys.* **35**(Part 2), L234–L236 (1996).
14. L. Dong, J. L. Archambault, L. Reekie, P. S. J. Russell, and D. N. Payne, "Bragg gratings in Ce³⁺-doped fibers written by a single excimer pulse," *Opt. Lett.* **18**(11), 861 (1993).
15. J. S. Stroud, "Photoionization of Ce³⁺ in Glass," *J. Chem. Phys.* **35**(3), 844–850 (1961).
16. H. Ebendorff-Heidepriem and D. Ehrt, "Formation and UV absorption of cerium, europium and terbium ions in different valencies in glasses," *Opt. Mater. (Amsterdam, Neth.)* **15**(1), 7–25 (2000).
17. X. Sun, J. Wen, Q. Guo, F. Pang, Z. Chen, Y. Luo, G. Peng, and T. Wang, "Fluorescence properties and energy level structure of Ce-doped silica fiber materials," *Opt. Mater. Express* **7**(3), 751 (2017).
18. L. Dong, P. J. Wells, D. P. Hand, and D. N. Payne, "Photosensitivity in Ce³⁺-doped optical fibers," *J. Opt. Soc. Am. B* **10**(1), 89 (1993).
19. J. Canning, "Photosensitization and Photostabilization of Laser-Induced Index Changes in Optical Fibers," *Opt. Fiber Technol.* **6**(3), 275–289 (2000).
20. M. Åslund, J. Canning, and G. Yoffe, "Locking in photosensitivity within optical fiber and planar waveguides by ultraviolet preexposure," *Opt. Lett.* **24**(24), 1826 (1999).
21. J. Fiebrandt, E. Lindner, S. Brückner, M. Becker, A. Schwuchow, M. Rothhardt, and H. Bartelt, "Growth characterization of fiber Bragg gratings inscribed in different rare-earth-doped fibers by UV and VIS femtosecond laser pulses," *Opt. Commun.* **285**(24), 5157–5162 (2012).
22. Y. Ishii, K. Arai, H. Namikawa, M. Tanaka, A. Negishi, and T. Handa, "Preparation of Cerium-Activated Silica Glasses: Phosphorus and Aluminum Codoping Effects on Absorption and Fluorescence Properties," *J. Am. Ceram. Soc.* **70**(2), 72–77 (1987).
23. B. Leconte, W. X. Xie, M. Douay, P. Bernage, P. Niy, J. F. Bayon, E. Delevaque, and H. Poignant, "Analysis of color-center-related contribution to Bragg grating formation in Ge:SiO₂ fiber based on a local Kramers-Kronig transformation of excess loss spectra," *Appl. Opt.* **36**(24), 5923–5930 (1997).
24. D. P. Hand and P. S. J. Russell, "Photoinduced refractive-index changes in germanosilicate fibers," *Opt. Lett.* **15**(2), 102–104 (1990).

25. P. Dekker, M. Ams, G. D. Marshall, D. J. Little, and M. J. Withford, "Annealing dynamics of waveguide Bragg gratings : evidence of femtosecond laser induced colour centres," *Opt. Express* **18**(4), 3274–3283 (2010).
26. M. J. F. Digonnet, "Kramers-Kronig analysis of the absorption change in fiber gratings," *Proc. SPIE* **2841**, 109–120 (1996).
27. F. Bilodeau, Y. Hibino, M. Abe, B. Malo, J. Albert, M. Kawachi, D. C. Johnson, and K. O. Hill, "Photosensitization of optical fiber and silica-on-silicon/silica waveguides," *Opt. Lett.* **18**(12), 953 (1993).
28. N. F. Borrelli, C. Smith, D. C. Allan, and T. P. S. Iii, "Densification of fused silica under 193-nm excitation," *J. Opt. Soc. Am. B* **14**(7), 1606–1615 (1997).
29. N. F. Borrelli, C. M. Smith, and D. C. Allan, "Excimer-laser-induced densification in binary silica glasses," *Opt. Lett.* **24**(20), 1401–1403 (1999).
30. M. Douay, W. X. Xie, T. Taunay, P. Bernage, P. Niay, P. Cordier, B. Poumellec, L. Dong, J. F. Bayon, H. Poignant, and E. Deleuaque, "Densification Involved in the UV-Based Photosensitivity of Silica Glasses and Optical Fibers," *J. Lightwave Technol.* **15**(8), 1329–1342 (1997).
31. B. Poumellec, P. Guénot, I. Riant, P. Sansonetti, P. Niay, P. Bernage, and J. F. Bayon, "UV induced densification during Bragg grating inscription in Ge:SiO₂ preforms," *Opt. Mater. (Amsterdam, Neth.)* **4**(4), 441–449 (1995).
32. R. Kashyap, "Chapter 2 – Photosensitivity and Photosensitization of Optical Fibers," in *Fiber Bragg Gratings* (Academic Press, 1999), pp. 13–54.
33. H. Hosono, M. Mizuguchi, H. Kawazoe, and J. Nishii, "Correlation between GeE' Centers and Optical Absorption Bands in SiO₂:GeO₂ Glasses," *Jpn. J. Appl. Phys.* **35**(Part 2), L234–L236 (1996).
34. A. Othonos, K. Kalli, and G. E. Kohnke, "Fiber Bragg Gratings: Fundamentals and Applications in Telecommunications and Sensing," *Phys. Today* **53**(5), 61–62 (2000).
35. B. Poumellec, "Links between writing and erasure (or stability) of Bragg gratings in disordered media," *J. Non-Cryst. Solids* **239**(1-3), 108–115 (1998).
36. B. Poumellec and M. Lancry, "Kinetics of Thermally Activated Physical Processes in Disordered Media," *Fibers* **3**(4), 206–252 (2015).
37. S. Unger, A. Schwuchow, S. Jetschke, S. Grimm, A. Scheffel, and J. Kirchhof, "Optical properties of cerium-codoped high power laser fibers," *Optical Components and Materials X* (2013) 8621, 862116.
38. S. Jetschke, S. Unger, A. Schwuchow, M. Leich, and M. Jäger, "Role of Ce in Yb/Al laser fibers: prevention of photodarkening and thermal effects," *Opt. Express* **24**(12), 13009 (2016).
39. L. Dong, J. Pinkstone, P. S. J. Russell, and D. N. Payne, "Ultraviolet absorption in modified chemical vapor deposition preforms," *J. Opt. Soc. Am. B* **11**(10), 2106 (1994).
40. B. Malo, J. Albert, F. Bilodeau, T. Kitagawa, D. C. Johnson, K. O. Hill, K. Hattori, Y. Hibino, and S. Gujrathi, "Photosensitivity in phosphorus-doped silica glass and optical waveguides," *Appl. Phys. Lett.* **65**(4), 394–396 (1994).
41. M. L. Brandily-Anne, J. Lumeau, L. Glebova, and L. B. Glebov, "Specific absorption spectra of cerium in multicomponent silicate glasses," *J. Non-Cryst. Solids* **356**(44-49), 2337–2343 (2010).
42. J. S. Stroud, "Color centers in a cerium-containing silicate glass," *J. Chem. Phys.* **37**(4), 836–841 (1962).
43. X. Fu, L. Song, and J. Li, "Radiation induced color centers in cerium-doped and cerium-free multicomponent silicate glasses," *J. Rare Earths* **32**(11), 1037–1042 (2014).